Localization of Cytoplasmic and Extracellular Domains of Na,K-ATPase by Epitope Tag Insertion†

Victor A. Canfield, Lauri Norbeck, and Robert Levenson*

Department of Pharmacology, Milton S. Hershey Medical Center, Penn State College of Medicine, P.O. Box 850, Hershey, Pennsylvania 17033

Received July 25, 1996; Revised Manuscript Received September 18, 1996⊗

ABSTRACT: We have used epitope tag addition to analyze the transmembrane topology of the Na,K-ATPase catalytic (α) subunit. An antigenic peptide derived from the hemagglutinin (HA) of influenza virus was inserted at 15 different positions within the rat Na,K-ATPase α1 subunit isoform. The functional integrity of the tagged proteins was tested by their capacity to confer ouabain resistance upon human HEK 293 cells. Constructs with the tag at aa positions 119, 173, 318, 815, 881, 953, 987, and 1023 conferred ouabain resistance, and the mutant proteins were detectable in the plasma membrane of transfected cells. In contrast, α1 subunits with insertions at aa positions 338, 797, 805, 868, 895, 910, and 921 were unable to confer drug resistance. Immunofluorescence analysis of permeabilized and intact cells using a monoclonal antibody specific for the HA epitope showed that double tags at positions 119 and 318 were located extracellularly, whereas single or double tags at positions 173, 815, 881, 987, and 1023 were cytoplasmically disposed. These results are consistent with an eight transmembrane domain arrangement for the α subunit. Epitope insertion within TM4, and the region linking transmembrane segments TM6−TM7, caused the loss of α subunit function, suggesting that the integrity of these domains is essential for the proper biosynthesis and/or maturation of the α subunit.

Na,K-ATPase is a membrane-associated enzyme that catalyzes the translocation of Na^+ and K^+ across the plasma membrane of most animal cells. Na,K-ATPase has been shown to consist of two subunits. The α subunit is a polypeptide of M_r ∼100 000 that contains the catalytic site for ATP hydrolysis and serves as the cellular receptor for cardiac glycosides such as ouabain and digitalis (Cantley, 1981). The β subunit is a glycosylated polypeptide of unknown function. Three separate genes, encoding three highly conserved α subunit isoforms, have been identified in rodents (Kent et al., 1987b). The cDNA for the rodent α1 subunit isoform has been shown to be capable of conferring ouabain resistance upon ouabain-sensitive primate cells in DNA transfection experiments (Kent et al.,1987a; Emanuel et al., 1988).

Understanding the overall structure of the Na,K-ATPase is a prerequisite for elucidating the relationship between enzyme structure and function. However, the topographical arrangement of Na,K-ATPase within the plasma membrane is still controversial. Based on hydropathy analysis of the predicted amino acid sequence, several secondary structure models have been proposed in which the α subunit has from 6 to 10 membrane spanning domains (Kawakami et al., 1985; Shull et al., 1985; Herrera et al., 1987; Takeyasu et al., 1990). The available experimental data suggest the following topology for the Na,K-ATPase α subunit: intracellular N- and C-termini (Felsenfeld & Sweadner, 1988; Canfield & Levenson, 1993; Thibault, 1993; Yoon & Guidotti, 1994), four hydrophobic transmembrane (TM) domains in the N-terminal portion of the molecule (Jørgenson et al., 1982; Ovchinnikov et al., 1988; Xie & Morimoto, 1995), and a large cytoplasmic loop connecting TM segments 4 and 5 (Farley et al., 1984; Ohta et al., 1985). However, the precise number and location of TM domains in the C-terminal region of the α subunit polypeptide have not been clearly established.

Sequence analysis of cloned cDNAs indicates that the Na,K-ATPase α subunit shares a high degree of structural homology with other cation-motive transporters including the sarcoplasmic reticulum Ca^{2+}-ATPase, the H,K-ATPase of mammalian stomach, and the plasmalemmal H^+-ATPase of yeast and fungi. A 10 TM model of the Ca^{2+}-ATPase has been inferred from image analysis of sarcoplasmic reticulum (Toyoshima et al., 1993), while analysis of microcrystals of detergent-solubilized Na,K-ATPase and Ca^{2+}-ATPase suggests that these enzymes share a similar three-dimensional structure (Taylor & Varga, 1994). *N*-Glycosylation site tagging has been used to localize TM domains in the *Neurospora* H^+-ATPase. Analyses of truncated H^+-ATPase reporter molecules translated *in vitro* and translocated into microsomes have suggested a 4 TM topology for the N-terminal portion and a 6 TM topology for the C-terminal region (Lin & Addison, 1995).

Biochemical and immunological methods have been used to analyze the topological organization of the C-terminal portion of the Na,K-ATPase α subunit. However, these approaches have yielded contradictory results. For example, tryptic digestion of microsomal vesicles revealed that a segment of the α subunit containing Asn-838 is localized intracellularly (Karlish et al., 1993). Similar results were obtained by immunohistochemical localization of an epitope tag situated at residue 832 (Canfield & Levenson, 1993). In contrast, epitope mapping with sequence-specific monoclonal

† This work was supported by NIH Grants HL-39263 and GM-49023 to R.L.

* Corresponding author. Telephone: (717) 531-4545. Fax: (717) 531-5013. Email: Levenson @neuro.hmc.psu.edu.

⊗ Abstract published in *Advance ACS Abstracts,* November 1, 1996.

S0006-2960(96)01851-X CCC: $12.00

antibodies and immunoelectron microscopy localized this domain (containing residues 817−832) to the extracellular side of the plasma membrane (Mohraz et al., 1994). A segment of the α subunit containing residues 894−911 was also placed extracellularly, leading to novel predictions regarding the localization of TM segments within the C-terminus of the polypeptide (Mohraz et al., 1994).

At present, it is difficult to resolve some of the discrepancies obtained among studies of the membrane topology of Na,K-ATPase. Some of these discrepancies may result from the use of *in vitro* systems that provide an incomplete or misleading picture of the native conformation of the polypeptide within a cell. To help resolve these issues, we developed a genetic approach to determine the topology of TM domains within an integral membrane protein (Canfield & Levenson, 1993; Kast et al., 1995, 1996). This approach is based on the expression in mammalian cells of polypeptides carrying an antigenic tag at defined locations, and determination of the intra- or extracellular location of the tags by immunofluorescence analysis. The application of this method is particularly useful for the Na,K-ATPase α1 subunit, because the biological activity of the mutant protein can be easily measured by transfection. The ability of an epitope-tagged α1 subunit to transfer ouabain resistance in this assay demonstrates that the polypeptide can form a functional Na,K-ATPase, and provides confidence that the structural integrity of the tagged protein has not been compromised.

We have previously used epitope addition to determine the location of the N- and C-termini of the Na,K-ATPase α subunit (Canfield & Levenson, 1993). Analysis of a series of tagged constructs provided an initial picture of the TM topology of the α subunit. Here we have used epitope insertion to more accurately define the location of intracellular and extracellular domains within the α subunit polypeptide. Our data are most consistent with an 8 TM model of α subunit topology.

EXPERIMENTAL PROCEDURES

DNA Constructs. (A) Single Tags. Epitope-tagged Na,K-ATPase α1 subunits were generated by introduction of a nine amino acid (aa) peptide (YPYDVPDYA) from the hemagglutinin (HA) of influenza virus into rat α1 subunit cDNA. Two strategies were used for the insertion of a single epitope tag. In the first, we generated a set of HA oligonucleotides that could be introduced in-frame into any natural or engineered blunt-ended restriction site in the cDNA (Canfield & Levenson, 1993). Using this method, oligonucleotide tags were introduced at aa positions 173, 318, 338, 921, 953, 987, and 1023 as outlined in Table 1. The second approach involved the use of PCR mutagenesis as described by Nelson and Long (1989). This method was used to insert a single tag at aa positions 119, 797, 805, 815, 868, 881, 895, and 910 (Table 1). Two variants of the α1 subunit cDNA containing a tag at residue 119 were constructed. In the first (HA119I), the HA tag was inserted between aa 119 and 120, thereby increasing the size of the first predicted extracellular loop by nine aa residues. In the second (HA119R), the HA epitope replaced aa residues 120−128, thereby maintaining the size of the first extracellular domain.

(B) Double Tags. Double-tagged constructs were generated from cDNAs carrying a single HA tag. Plasmids encoding the 5′ half-tag (5′-GAGCTCG**TACCCATAC-GACGTC**-3′) and the 3′ half-tag (5′-**GACGTC**CCAGAC **TACGC**GAGCTC-3′) were constructed so that the HA epitope tag sequences (boldface) in the two plasmids overlap at a common *Aat*II site (underlined) and are flanked by *Sac*I sites (double underline). The 3′ half- and 5′ half-tag plasmids were ligated separately to the 5′ and 3′ segments of constructs carrying a single tag. The resulting plasmids were then joined at the *Sac*I site to generate double-tagged inserts. This method was used to create double tags at aa positions 14, 119, 318, 815, 881, and 953. Each single- and double-tagged mutant α1 subunit was verified by dideoxynucleotide sequencing, and then subcloned into the eukaryotic expression vector pCB6.

Cell Culture and DNA Transfection. Human embryonic kidney (HEK) 293 cells were used as recipients for transfection. Cells were grown in Dulbecco's modified Eagle's medium (DMEM) supplemented with 10% fetal calf serum (FCS). Transfections were performed by the calcium phosphate coprecipitation method as previously described (Kent et al., 1987a; Canfield & Levenson, 1993). For stable transfectants, cultures were split 1:4 48 h after transfection, and medium containing ouabain (0.5 μM) was added 4 h later. Colonies of transfected cells were picked in 2−3 weeks and expanded into cell lines that were maintained in medium containing 0.5 μM ouabain. For transient transfection, HEK 293 cells were plated on glass coverslips and transfected under the conditions described above.

Membrane Preparation and Immunoblotting. Crude membrane fractions from stably transfected HEK 293 cells were prepared as described previously (Shyjan & Levenson, 1989), and protein concentrations were determined by the method of Bradford (1976). Solubilized membrane fractions were fractionated on an SDS-containing 7.5% polyacrylamide gel (50 μg of protein/lane) and transferred to a nitrocellulose filter as described (Towbin et al., 1979). The filter was quenched overnight in Tris-buffered saline (TBS) containing 5% dry milk and 0.1% Tween 20 and then incubated with the HA-specific monoclonal antibody (mAb) 12CA5 (Wilson et al., 1984) (Babco Labs, Richmond, CA). The filter was rinsed with TBS, 0.1% Tween 20, and then incubated with horseradish peroxidase conjugated goat anti-mouse (second) antibody for 1 h. Immunoreactivity was detected by enhanced chemiluminescence (ECL) using an ECL kit (Amersham).

Immunofluorescence and Confocal Microscopy. Transiently transfected HEK 293 cells grown on coverslips were examined 72 h after transfection. For experiments using permeabilized cells, HEK 293 cells were fixed in 4% paraformaldehyde in phosphate-buffered saline (PBS). Cells were permeabilized and blocked with 0.05% Nonidet P-40 in PBS, 5% goat serum, and 1% bovine serum albumin at room temperature for 15 min and then incubated in the same medium containing the 12CA5 mAb (diluted 1:500) for 1 h. Secondary antibody (Texas-Red-conjugated rabbit anti-mouse IgG) was diluted 1:200 and applied in the same buffer. Nonpermeabilized HEK 293 cells were incubated with mAb 12CA5 in DMEM, 10% FCS, and 20 mM HEPES, pH 7.2 at 4 °C, for 1 h. Cells were fixed, permeabilized, and incubated with secondary antibody as described above. Immunofluorescence microscopy was performed using standard epifluorescence optics (Olympus Bmax 50) or by

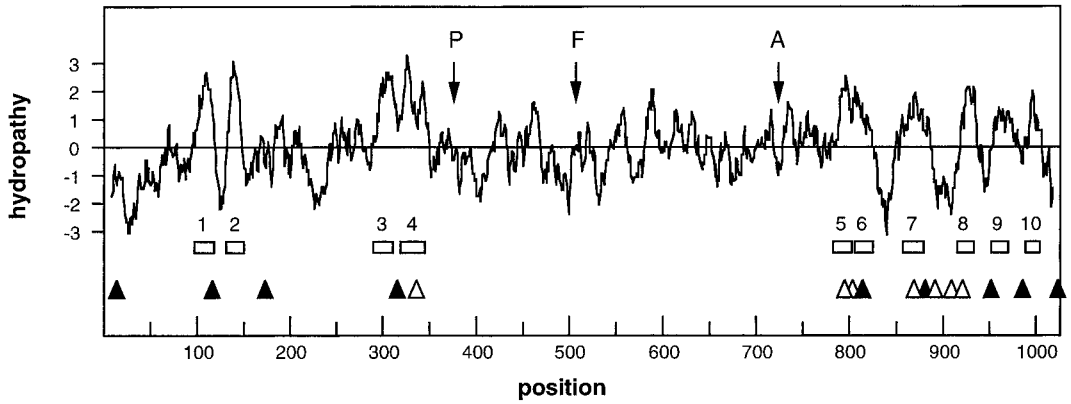

FIGURE 1: Schematic representation of HA epitope insertions used to determine Na,K-ATPase α subunit topology. Hydropathy analysis of the α1 subunit calculated by the algorithm of Kyte and Doolittle (1982). Predicted TM domains are indicated by open boxes numbered 1−10. Insertion sites of the HA epitope tag are identified by solid (epitope-tagged constructs capable of conferring ouabain resistance) or open (epitope-tagged constructs that do not confer drug resistance) triangles. The phosphorylation (P), FITC-reactive (F), and FSBA-reactive (A) sites are indicated by arrows. The scale (every 100 aa) is shown at the bottom.

confocal laser scanning microscopy using a Zeiss LSM 210 confocal microscope (Rh filter block, 543-nm excitation wavelength).

RESULTS

Construction and Expression of Epitope-Tagged Na,K-ATPase α1 cDNAs. To analyze the TM topology of the Na,K-ATPase, we determined the intra- versus extracellular location of an HA epitope tag inserted at various sites within the expressed α1 subunit polypeptide. As shown in Figure 1, single epitope tags were inserted within the predicted first and second extracellular domains at aa positions 119 and 318, respectively. To determine the location of the predicted third extracellular domain, three separate tags were inserted at aa positions 797, 805, and 815. A single tag was also introduced at aa position 953, a site predicted to reside within the fourth extracellular domain. An HA epitope tag was inserted in the first predicted intracellular loop (after TM2) at aa position 173, and at aa position 338, a site within predicted TM4. To localize TM 7, epitope tags were inserted at aa positions 868, 881, 895, 910, and 921. These residues are contained within a hydrophilic region situated between potential TM segments 7 and 8 (Figure 1) at positions 852−879 and 916−936. Single HA tags were also inserted at aa positions 987 and 1023 to analyze the topology of the C-terminal segment of the α1 subunit.

To test biological activity, each of the epitope-tagged α1 subunits was transfected into ouabain-sensitive HEK 293 cells, and transfected cells were tested for their ability to proliferate in 0.5 μM ouabain. We have previously shown that this concentration of drug is cytotoxic to HEK 293 cells (Canfield & Levenson, 1993). Wild-type rat α1 subunit cDNA was transfected into HEK 293 cells as a positive control. Constructs HA119I, HA119R, HA173, HA318, HA815, HA881, HA953, HA987, and HA1023, containing the HA tag at aa positions 119, 173, 318, 815, 881, 953, 988, and 1023, respectively, produced ouabain-resistant colonies (Table 1). In general, epitope-tagged constructs gave ouabain-resistant colonies with an efficiency similar to that of the wild-type rat α1 subunit. The ability of these epitope-tagged constructs to confer ouabain resistance to HEK 293 cells indicates that the mutant α1 subunit polypeptides are capable of forming a functional Na,K-ATPase. Immunoblot analysis of membrane fractions prepared from ouabain-resistant clones revealed the presence of epitope-tagged α1 subunits in all transfectants (data not shown). Constructs carrying the HA epitope tag at aa positions 338, 797, 805, 868, 895, 910, and 921 failed to confer ouabain resistance in our assay (Table 1). The presence of epitopes at these sites may interfere with the proper membrane insertion or folding of the α1 subunit.

Table 1: Biological Activity of α1 Subunits Carrying a Single Epitope Tag

mutant	sequence[a]	resistant colonies[b]
HA14	A14-V(tag)A-V15	+
HA119R[c]	R119-(tag)-D129	+
HA119I[d]	R119-(tag)-S120	+
HA173	R173-(tag)-N174	+
HA318	L318-D(tag)AV-E319	+
HA338	A338-V(tag)AA-T339	−
HA797	A796-(tag)-N797	−
HA805	V805-T(tag)TV-T806	−
HA815	D815-(tag)D-M816	+
HA881	F881-(tag)F-H882	+
HA868	T868-(tag)-Y869	−
HA895	I895-(tag)-N896	−
HA910	Q910-(tag)Q-R911	−
HA921	A921-(tag)AAA-F922	−
HA953	I953-(tag)AI-L954	+
HA987	S986-(tag)A-W988	+
HA1023[e]	Y1023-C(tag)	+

[a] Mutations were introduced into the rat α1 subunit at the amino acid positions indicated (numbered from the initiating methionine). The amino acid sequence flanking the HA epitope (tag = YPYDVPDYA) is indicated using the single-letter amino acid code. Additional residues specific for each construct are shown flanking the tag. [b] HEK 293 cells were transfected with mutant cDNAs and selected in the presence of 0.5 μM ouabain. [c] HA epitope replaced residues 120−128. [d] HA epitope added nine residues to the first extracellular loop. [e] The tag in HA1023 is followed by a stop codon.

Localization of Epitope Tags. The membrane polarity of the HA tags (cytoplasmic versus extracellular) was determined by immunofluorescence analysis of HEK 293 cells transiently expressing epitope-tagged α1 subunits. Stable and transient expression of the epitope-tagged constructs gave identical patterns of immunoreactivity. However, transient expression facilitates detection of the epitope-tagged constructs due to the higher levels of tagged protein produced compared to stably transfected cells (Canfield & Levenson, 1993). The orientation of the tag with respect to its intracellular versus extracellular localization was determined

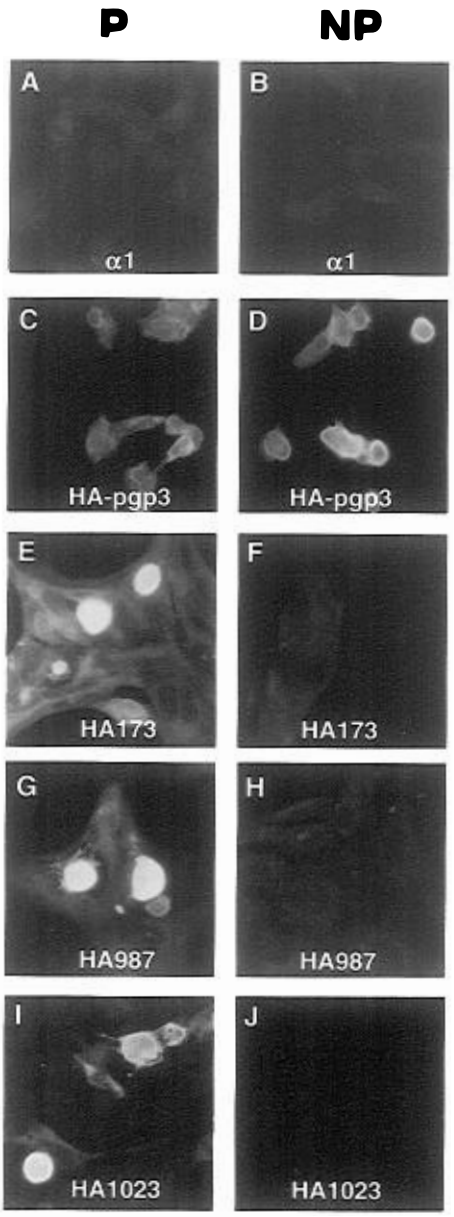

FIGURE 2: *In situ* detection of epitope-tagged α1 subunits by immunofluorescence. HEK 293 cells transiently expressing epitope-tagged rat α1 subunit cDNAs were examined for 12CA5 mAb reactivity 3 days after transfection. For each construct, representative fields of permeabilized (P, left column) or nonpermeabilized (NP, right column) cells are shown. Cells expressing wild-type rat α1 subunits (A, B) were not reactive with the 12CA5 mAb, whereas an epitope-tagged mouse *mdr3* P-glycoprotein was visualized in both permeabilized and nonpermeabilized cells (C, D). The single epitope tags in constructs HA173 (E, F), HA987 (G, H), and HA1023 (I, J) were detected only in permeabilized cells.

by immunofluorescence microscopy on intact cells (extracellular) or on cells permeabilized with Nonidet P-40 (intracellular). Representative examples of cells expressing each tagged α1 subunit polypeptide are shown in Figure 2. HEK 293 cells transfected with wild-type (untagged) rat α1 subunit cDNA were not immunoreactive with mAb 12CA5 in either permeabilized or intact cells (Figure 2A,B). As a positive control for detection of an extracellular tag, we monitored immunoreactivity of an expressed P-glycoprotein (mouse *mdr3*) carrying an HA epitope tag in the first extracellular domain (Kast et al., 1995). The 12CA5 mAb specifically detected the epitope-tagged *mdr3* polypeptide in both permeabilized and nonpermeabilized HEK 293 cells (Figure 2C,D), demonstrating the extracellular localization of the HA epitope in this fusion protein. In HEK 293 cells expressing the HA173, HA987, and HA1023 constructs, the 12CA5 mAb specifically detected each of the tagged proteins in permeabilized but not nonpermeabilized cells (Figure 2E−J), suggesting the intracellular localization of these epitope-tagged regions. However, epitope-tagged constructs HA119I, HA119R, HA318, HA815, HA881, and HA953 were undetectable in either detergent-treated or intact cells (data not shown). Failure to detect the HA epitope by immunofluorescence suggests that the tag is situated in a region of the protein that is inaccessible to mAb 12CA5.

Table 2: Biological Activity of α1 Subunits Carrying a Double Epitope Tag

mutant	sequence[a]	resistant colonies[b]
HA(2x)14	A14-V(tag)SS(tag)AV-S15	+
HA(2x)119R	R119-(tag)SS(tag)-D129	+
HA(2x)119I	R119-(tag)SS(tag)-S120	+
HA(2x)318	L318-D(tag)SS(tag)AV-E319	+
HA(2x)815	D815-(tag)SS(tag)D-M816	−
HA(2x)881	F881-(tag)SS(tag)F-H882	+
HA(2x)953	I953-(tag)AI(tag)AI-L954	−

[a] Mutations were introduced into the rat α1 subunit at the residues indicated (numbered from the initiating methionine). Additional residues specific for each construct are shown flanking the HA epitope (tag). [b] HEK 293 cells were transfected with mutant cDNAs and selected in the presence of 0.5 μM ouabain.

Expression of Double-Tagged Constructs. To visualize tagged segments within the α1 subunit where the HA epitope may be masked from the 12CA5 antibody, we adopted a strategy of introducing a second copy of the HA tag into the mutant proteins. This strategy was based on the assumption that a tandem duplication of the HA tag should increase the immunoreactivity or accessibility of the tags to mAb 12CA5, thereby improving the immunofluorescence signal. This approach has been successfully used to detect epitope-tagged P-glycoprotein (Kast et al., 1996). Double HA tags were introduced into the α1 subunit at aa positions 14, 119, 318, 815, 881, and 953, respectively (Table 2). Each of the constructs was transfected into HEK 293 cells and tested for the ability to transfer ouabain resistance. As shown in Table 2, double-tagged constructs HA(2x)14, HA(2x)-119R, HA(2x)119I, HA(2x)318, and HA(2x)881 conferred ouabain resistance upon HEK 293 cells. In contrast, constructs HA(2x)815 and HA(2x)953 failed to transfer drug resistance, suggesting that the presence of a double tag at these positions abrogates the proper function of the α1 subunit. Western blot analysis of crude membrane fractions prepared from stable ouabain-resistant colonies transfected with constructs HA(2x)14, HA(2x)119I, HA(2x)318, and HA(2x)881 showed the presence of a 12CA5 immunoreactive band of ∼100 kDa which is absent from control cells (Figure 3). Immunofluorescence analysis of stably transfected HEK 293 cells expressing each of the double-tagged mutant α1 subunits is shown in Figure 4. As expected, the HA(2x)14 double tag was only detectable in permeabilized cells (Figure 4A,B). No apparent increase in immunofluorescence was detected in the double-tagged polypeptide compared to the single tag construct HA14 (Figure 4C). Examination of HEK 293 cells expressing the HA(2x)119I and HA(2x)318 constructs revealed 12CA5 reactivity in both permeabilized (Figure 4D,G) and intact cells (Figure 4E,H), indicating an extracellular localization of the 12CA5 reactive

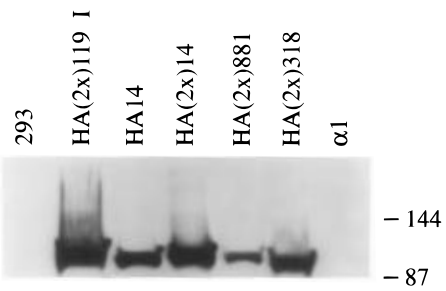

FIGURE 3: Immunoblot analysis of double-tagged α1 subunits expressed in HEK 293 cells. Crude membranes were prepared from stable HEK 293 cell clones transfected with double-tagged or wild-type rat α1 subunit cDNAs. Solubilized microsomal proteins (30 μg/lane) were resolved on an SDS-containing 7.5% polyacrylamide gel, transferred to a nitrocellulose filter, and probed with the HA epitope-specific mAb 12CA5. Immunoreactivity was detected by ECL. Positions of the molecular mass markers (in kDa) are shown at the right.

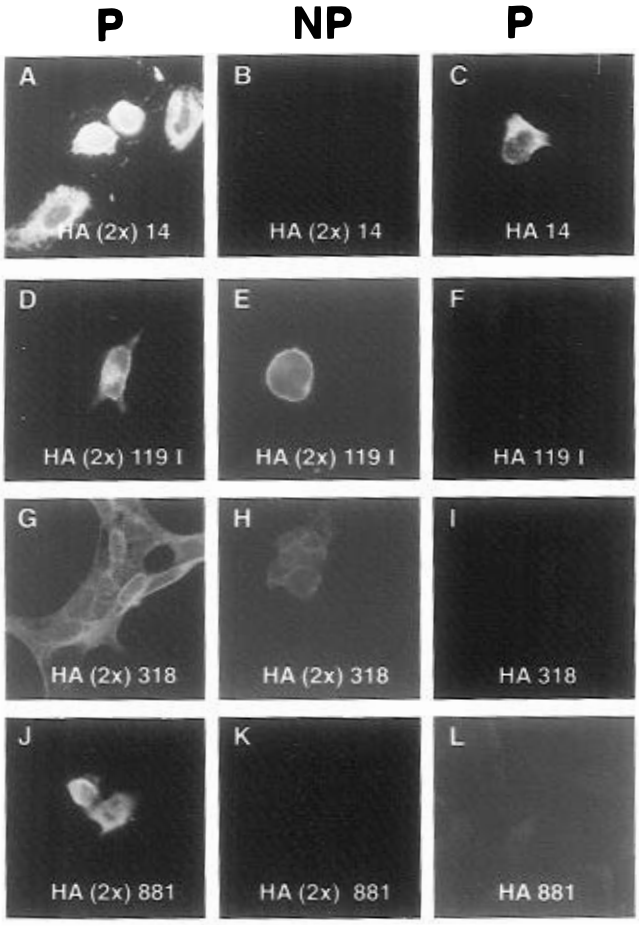

FIGURE 4: *In situ* immunofluorescence analysis of α1 subunits carrying double HA tags. HEK 293 cells stably transfected with double-tagged α1 subunit cDNAs were examined for mAb 12CA5 immunoreactivity. The double-tagged constructs HA(2x)14 (A, B) and HA(2x)881 (J, K) were detected only in permeabilized cells. Constructs HA(2x)119I (D, E) and HA(2x)318 (G, H) were visualized in both permeabilized (P) and nonpermeabilized (NP) cells. Permeabilized HEK 293 cells expressing the single-tagged constructs HA14 (C), HA119I (F), HA318 (I), and HA881 (L) are shown for comparison.

epitope at position 119. No detectable immunofluorescence was observed in cells expressing the single tag constructs HA119I (Figure 4F) or HA318 (Figure 4I). These results are consistent with the proposed extracellular distribution of the loops situated between TM1−2 and TM3−4 (Ovchinnikov et al., 1988; Mohraz et al., 1994; Yoon & Guidotti, 1994). In HEK 293 cells expressing the double-tagged construct HA(2x)881, 12CA5 mAb reactivity was detectable only in permeabilized cells (Figure 4J,K), indicating that the tag at residue 881 is localized intracellularly. The double tag gave a substantial increase in fluorescence compared to the single tag in construct HA881 (Figure 4L).

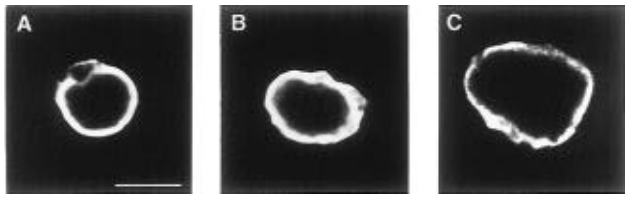

FIGURE 5: Visualization of epitope-tagged α1 subunits by confocal laser microscopy. HEK 293 cells expressing the single tag construct HA1023 (A) and the double-tagged constructs HA(2x)14 (B) and HA(2x)881 (C) were fixed and permeabilized. The HA epitope was detected using the 12CA5 mAb and Texas Red-conjugated anti-mouse antibodies. Optical sections were scanned through cells ~2 μm above the coverslip. Scale bar = 10 μm.

Confocal microscopy was used to more precisely determine the subcellular distribution of epitope-tagged α1 subunits. Results of these studies for the single tag construct HA1023 and the double tag constructs HA(2x)14 and HA(2x)881 are shown in Figure 5. Examination of HEK 293 cells transiently expressing these constructs revealed in each case bright staining at cell margins. These results are consistent with a predominantly plasma membrane localization of the expressed proteins.

DISCUSSION

We have used epitope tag addition to investigate the topographical organization of the Na,K-ATPase α1 subunit. The utility of this method derives from several considerations. Localization of the epitope tag is performed on intact cells expressing full-length protein. The biological assay is dependent on the ability of the tagged α1 subunit to confer ouabain resistance, thus providing confidence that the structural integrity of the tagged protein has not been compromised. The assay is carried out in mammalian cells which provide a normal physiological background where proper posttranslational modification can take place, and finally, the plasma membrane association of the tagged protein can be demonstrated by confocal microscopy. The rat Na,K-ATPase α1 subunit therefore serves as a useful model for testing computational predictions of membrane topology.

A model of α1 subunit topology suggested by our epitope tagging experiments is shown in Figure 6. Direct examination of cells expressing the double-tagged constructs HA(2x)119I and HA(2x)318 shows that in each case the 12CA5 mAb reacts with nonpermeabilized cells, whereas the mAb reacts only with permeabilized cells expressing the single-tagged construct HA173. These results indicate that the segments linking TM1−2 and TM3−4 are extracellular while the segment linking TM2−3 is intracellular. The localization of these epitope-tagged polypeptides therefore allows the unambiguous positioning of one intracellular and two extracellular loops and confirms the presence of four TM domains (TM1−4) in the N-terminal region of the α1 subunit. These results are in good agreement with previous predictions of the transmembrane organization of the N-

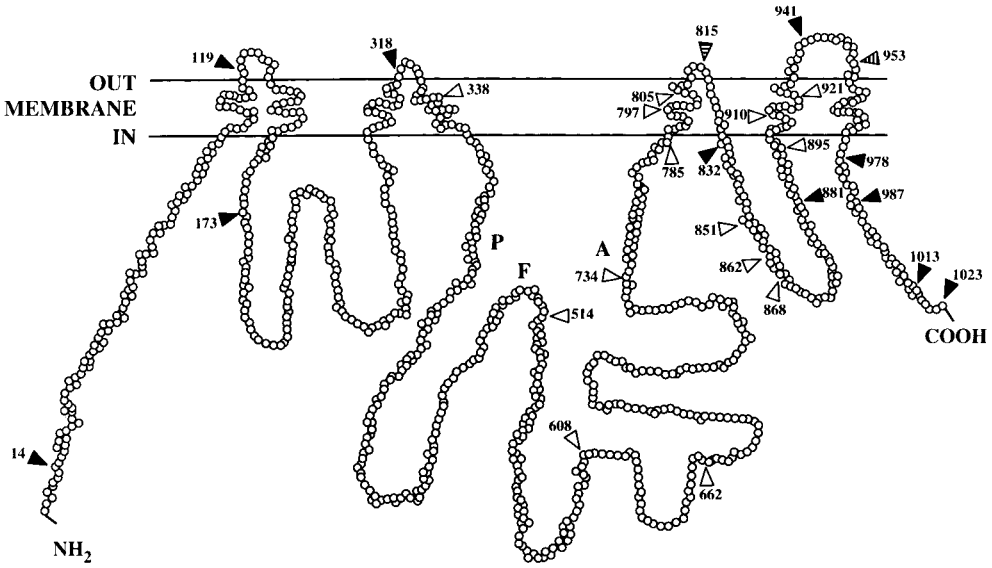

FIGURE 6: Proposed membrane topology of the Na,K-ATPase α1 subunit. Topology is based on the immunolocalization of single and double HA epitope tags. Epitope tagging experiments are consistent with the presence of eight TM segments, with the amino (N) and carboxyl termini (C) disposed cytoplasmically. Insertion sites of the HA epitope are numbered and indicted by triangles. Solid triangles denote constructs capable of transferring ouabain resistance whereas open triangles represent constructs that did not confer the drug-resistant phenotype. Hatched triangles designate constructs that conferred ouabain resistance but were not visible by immunofluorescence. The phosphorylation (P), FITC-reactive (F), and FSBA-reactive (A) sites are indicated. Folding of intracellular loops is for artistic purposes only and does not imply secondary structural features of the molecule.

terminal portion of the α subunit (Jørgenson et al., 1982; Ovchinnikov et al., 1988; Xie & Morimoto, 1995).

Hydropathy analysis of the α1 subunit sequence identifies a long hydrophobic segment (38 residues) situated between residues 787 and 824. Current models of α subunit topography have assigned two TM domains to this segment (Canfield & Levenson, 1993; Yoon & Guidotti, 1994), although this topographical arrangement has not been firmly established. The positioning of the third extracellular loop and predicted TM domains 5 and 6 was attempted by introduction of HA tags at aa positions 797, 805, and 815. However, insertion of the HA tag at positions 797 and 805 resulted in nonfunctional proteins that could not be analyzed. Introduction of a single tag at residue 815 produced a mutant α1 subunit that was capable of transferring ouabain resistance. Unfortunately, we were unable to visualize the single-tagged HA815 polypeptide by immunofluorescence, and introduction of a double tag at residue 815 produced a nonfunctional α1 subunit. Thus, we have been unable to directly determine the position of TM segments 5 and 6 or verify the presence of an extracellular loop linking these TM domains. However, our demonstration that it is possible to introduce a single tag at position 815 without the loss of α subunit function strongly suggests that residue 815 is not embedded within the lipid bilayer. Epitope mapping using a monoclonal antibody indicates that a portion of the segment spanning residues 817−832 is situated extracellularly (Mohraz et al., 1994). Since the region in the vicinity of residue 832 has been mapped intracellularly (Canfield & Levenson, 1993; Karlish et al., 1993; Yoon & Guidotti, 1994), these results taken together are most consistent with an extracellular localization for residue 815. Regardless of whether residue 815 is disposed extracellularly or intracellularly, the bridge between TM segments 5 and 6 would have to be relatively short in order to accommodate two membrane-spanning segments in this region. This type of arrangement also predicts that TM segments 5 and 6 are relatively short (<19 aa in length), thus raising the possibility that TM segments 5 and 6 may not form typical α-helical structures. Alternatively, TM segments 5 and 6 may form a hairpin within a proteinaceous portion of the membrane. Such an arrangement has been proposed for the pore region of voltage-activated K^+ channels (Jan & Jan, 1992).

Hydropathy analysis of the α1 subunit identifies two potential TM domains situated between residues 852−879 and 916−936. However, our previous localization studies (Canfield & Levenson, 1993) indicated an odd number of TM segments in this region. To localize TM domains in this region, epitope tags were inserted at residues 868, 881, 895, 910, and 921. Mutant α1 subunits carrying the tag at aa positions 868, 895, 910, and 921 were nonfunctional and could not be analyzed. The single-tagged HA881 construct produced a functional α1 subunit which could not be visualized with the 12CA5 mAb. However, α1 subunits containing a double tag at residue 881 transferred ouabain resistance, and the tag was localized intracellularly by immunofluorescence microscopy. The intracellular localization of the tag at aa 881, coupled with the extracellular localization of residue 941 (Canfield & Levenson, 1993), would then position TM7 between residues 881 and 941.

To further characterize the C-terminal segment of the α1 subunit, single epitope tags were inserted at aa positions 953, 987, and 1023. Each of the mutant polypeptides was capable of transferring ouabain resistance, and the tags at residues 987 and 1023 were situated intracellularly. These results confirm the cytoplasmic disposition of the C-terminus of the α1 subunit and suggest the presence of one TM segment between aa 941 and the C-terminus of the polypeptide. Taken together, our mapping studies are most consistent with an eight transmembrane segment model of α1 subunit topology.

A comparison of various models of α subunit structure is depicted in Figure 7. Hydropathy and biochemical analysis has suggested that the Na,K-ATPase α subunit contains either

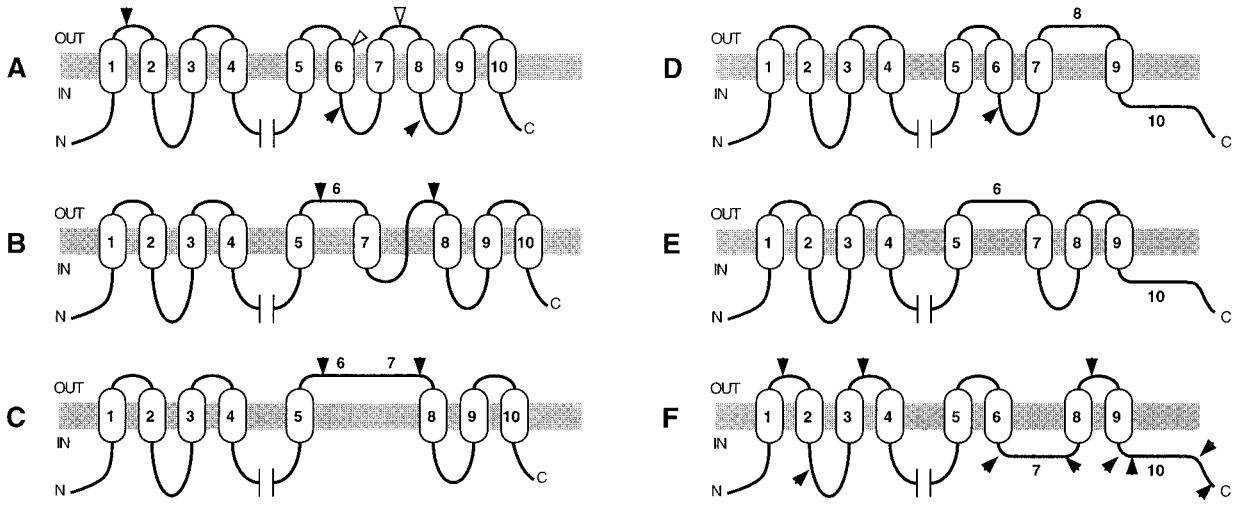

FIGURE 7: Proposed models of Na,K-ATPase α subunit topology. Transmembrane segments are represented by ovals, while the remainder of the polypeptide is represented by a solid line. The large cytoplasmic domain is omitted. In order to facilitate comparison of models, corresponding hydrophobic segments of the polypeptide are numbered 1−10. Panel A, 10 transmembrane segment hydropathy-based model (Takeyasu et al., 1990; Yoon & Guidotti, 1994; Karlish et al., 1993; Mohraz et al., 1994). Solid arrowheads indicate the positions of HA epitope insertions (Yoon & Guidotti, 1994), while open arrowheads indicate antibody-reactive epitopes (Mohraz et al., 1994). Panels B and C, 10 and 8 transmembrane segment models of Mohraz et al. (1994). Arrowheads indicate antibody-reactive epitopes. Panel D, 8 transmembrane segment model of Karlish et al. (1993). The arrowhead indicates the position of the trypsin-sensitive site. Panel E, 8 transmembrane segment, hydropathy-based model of Shull et al. (1985). Panel F, 8 transmembrane segment model predicted by HA epitope insertions (Canfield & Levenson, 1993; this study). Positions of HA insertions are indicated by arrowheads. Hydrophobic segments 7 and 10 are not membrane-spanning in this model.

8 (Shull & Lingrel, 1985; Figure 7E) or 10 (Takeyasu et al., 1990; Figure 7A) transmembrane segments. However, experimental localization of segments of the α subunit has appeared to support several alternative models containing 10 TM segments (Figure 7A, Karlish et al., 1993; Figure 7A, Yoon & Guidotti, 1994; Figure 7A−B, Mohraz et al., 1994) or 8 TM segments (Figure 7C, Mohraz et al., 1994; Figure 7D, Karlish et al., 1993; Figure 7F, this paper). The demonstrated intracellular localization of the N- and C-termini of the Na,K-ATPase α1 subunit indicates that there must be an even number of transmembrane segments within the α subunit polypeptide. The intracellular localization of the HA tags at residues 978, 987, 1013, and 1023 (Canfield & Levenson, 1993; data presented here) appears to be incompatible with the presence of the potential 10th transmembrane segment (situated between residues 986−1001) predicted by hydropathy. This localization of the carboxy terminus is compatible with the models depicted in Figure 7D−F but not with those shown in Figure 7A−C. To accommodate an even number of transmembrane segments, an additional hydrophobic segment must not span the membrane. The intracellular localization of tags inserted at residues 832 and 881 (Canfield & Levenson, 1993) suggests that the seventh hydrophobic segment situated between residues 849 and 874 is intracellular and not membrane-spanning (Figure 7F).

The eight-transmembrane model of α subunit topology presented in this study is based on the intra- versus extracellular localization of immunoreactive HA epitope tags inserted into an expressed Na,K-ATPase α1 subunit. We assigned residue 941 to an extracellular segment of the α subunit based on the visualization of the HA tag in nonpermeabilized cells (Canfield & Levenson, 1993). In contrast, an HA tag inserted at residue 944 was localized intracellularly (Yoon & Guidotti, 1994) as shown in Figure 7A. Our eight-transmembrane segment model also assigns residues 894−921 intracellularly (Figure 7F). This segment has been proposed to be extracellular (Mohraz et al., 1994; Figure 7B,C) and may constitute a site of α/β subunit interaction (Lemas et al., 1994). However, we have been unable to precisely localize this region since epitope tags inserted at positions 895, 910, and 921 produced α subunits that failed to transfer ouabain resistance. Independent methods for verifying the intra- versus extracellular localization of these regions will clearly be required to resolve these discrepancies.

Epitope tagging has proven to be a useful method for analyzing the transmembrane organization of the Na,K-ATPase. An important feature of this method is the ability to generate a tagged protein that retains biological activity. This property allows topographical analysis of a polypeptide whose overall structure has not been significantly altered. In some cases, however, addition of the epitope tag abrogates the proper function of the polypeptide. In such cases, the topology of the tagged domains cannot be accurately determined since insertion of the tag may lead to production of a polypeptide that is incorrectly folded or improperly processed. Thus, this method may not be applicable to all intracellular or extracellular domains of a polypeptide. Alternative approaches, such as cysteine replacement (Loo & Clarke, 1995), may provide a useful and complementary strategy for determining the polarity of membrane segments that do not tolerate epitope tag insertion. On the other hand, the epitope tag insertion protocol has proven useful for identifying regions of the protein in which structural integrity is absolutely essential for proper enzymatic function. For example, we have previously shown that insertion of the HA epitope within the second intracellular loop of the α1 subunit, in proximity to sites implicated in ATP binding, produces polypeptides that fail to transfer ouabain resistance (Canfield & Levenson, 1993). Here we show that insertion of the HA epitope directly into TM4, and the loop linking TM6−7, also produced nonfunctional α1 subunits. Further scanning with additional epitope insertions may help to more precisely

delineate regions within the α1 subunit that are essential for enzymatic function.

The ability to visualize an epitope tag and determine its intra- or extracellular location is a critical step in analyzing the membrane topology of a protein. Achieving high expression levels of the of the tagged protein facilitates this analysis. For example, epitope-tagged P-glycoprotein gives a very strong fluorescence signal, even in stably transfected cells, due to the amplification and overexpression of the murine *mdr3* gene (Kast et al., 1995, 1996). For the epitope-tagged Na,K-ATPase α1 subunit, the fluorescence signal obtained in stable transfectants was generally weak. Transient expression was therefore used to detect tagged α1 subunits because quantitatively higher levels of the tagged protein were produced by this method compared to stably transfected cells. However, for several of the single-tagged constructs (HA119, HA318, HA815, HA881, HA953), the HA epitope was not detectable using standard epifluorescence optics or confocal laser microscopy. Several potential explanations could account for these results. One possibility is that the epitope tag may be buried within the native protein, or be masked by sugar moieties, thus reducing the availability of the HA epitope for the 12CA5 mAb. Alternatively, if the tag is inserted in short loops, steric hindrance may prevent epitope−antibody interaction. Insertion of double HA tags provided a useful method for increasing the fluorescence signal and detection of the epitope tag with the HA-specific mAb. Using this approach, we were able to determine the extracellular localization of tags at residues 119 and 318, and the cytoplasmic location of a tag at residue 881. Insertion of double tags at residue 815 and 953 produced nonfunctional proteins, suggesting that there are sites within the protein that cannot tolerate the 18 amino acid insertion.

Our results raise interesting questions regarding the relationship between the structural integrity of extracellular domains and α1 subunit function. For example, the first extracellular loop of the α subunit has been shown to play an important role in determining the ouabain sensitivity of the Na,K-ATPase (Price & Lingrel, 1988; Emanuel et al., 1989; Canfield et al., 1990). The 2 residues situated at the boundaries of this 12 aa-long loop are responsible for both species- and isoform-specific differences in ouabain sensitivity. Here we show that replacement of 9 of 12 of the amino acids in the first extracellular loop produced a ouabain-resistant fusion protein. Increasing the size of the first extracellular loop to 21, 23, or 32 residues (by insertion of single or double HA tags) also produced a ouabain-resistant α1 subunit. These results indicate that the size constraints placed on this loop are fairly loose, and that the overall structure of this domain does not significantly contribute to the proper function of the Na,K-ATPase. Insertion of a single or double HA tag into the extracellular loop connecting TM3−4 increased the size of this loop from 5 to 14 or 25 residues in length, respectively. Using our transfection assay, we showed that both of these α1 subunit fusion proteins were capable of conferring ouabain resistance upon HEK 293 cells. Taken together, these results indicate that amino acid insertions within the first or second extracellular loops of the α1 subunit do not have a deleterious effect on the packing of the adjacent TM domains in the final three-dimensional structural arrangement of the protein.

REFERENCES

Bradford, M. M. (1976) *Anal. Biochem. 72,* 248−254.

Canfield, V. A., & Levenson, R. (1993) *Biochemistry 32,* 13782−13786.

Canfield, V., Emanuel, J. R., Spickofsky, N., Levenson, R., & Margolskee, R. (1990) *Mol. Cell. Biol. 10,* 1367−1372.

Cantley, L. C. (1981) *Curr. Top. Bioenerg. 11,* 201−237.

Emanuel, J. R., Schulz, J., Zhou, X.-M., Kent, R. B., Housman, D., Cantley, L., & Levenson, R. (1988) *J. Biol. Chem. 263,* 7726−7733.

Emanuel, J. R., Graw, S., Housman, D., & Levenson, R. (1989) *Mol. Cell. Biol. 9,* 3744−3749.

Farley, R. A., Tran, C. M., Carilli, C. T., Hawke, D., & Shively, J. E. (1984) *J. Biol. Chem. 259,* 9532−9535.

Felsenfeld, D. P., & Sweadner, K. J. (1988) *J. Biol. Chem. 263,* 10932−10942.

Herrera, V. L. M., Emanuel, J. R., Ruiz-Opazo, N., Levenson, R., & Nadal-Ginard, B., (1987) *J. Cell Biol. 105,* 1855−1865.

Jan, L. Y., & Jan, Y. N. (1992) *Annu. Rev. Physiol. 54,* 537−555.

Jørgenson, P. L., Karlish, S. J. D., & Gitler, C. (1982) *J. Biol. Chem. 257,* 7435−7442.

Karlish, S. J. D., Goldschleger, R., & Jørgenson, P. (1993) *J. Biol. Chem. 268,* 3471−3478.

Kast, C., Canfield, V., Levenson, R., & Gros, P. (1995) *Biochemistry 34,* 4402−4411.

Kast, C., Canfield, V., Levenson, R., & Gros, P. (1996) *J. Biol. Chem. 271:* 9240−9248.

Kawakami, K., Noguchi, S., Noda, M., Takahashi, H., Ohta, T., Kawamura, M., Nojima, H., Nagano, K., Hirose, T., Inayama, S., Hayashida, H., Miyata, T., & Numa, S. (1985) *Nature 316,* 733−736.

Kent, R. B., Emanuel, J. R., Neriah, Y. B., Levenson, R., & Housman, D. E. (1987a) *Science 237,* 901−903.

Kent, R. B., Fallows, D. A., Geissler, E., Glaser, T., Emanuel, J. R., Lalley, P., Levenson, R., & Housman, D. (1987b) *Proc. Natl. Acad. Sci. U.S.A. 84,* 5369−5373.

Kyte, J., & Doolittle, R. F. (1982) *J. Mol. Biol. 157,* 105−132.

Lemas, M. V., Hamrick, M., Takeyasu, K., & Fambrough, D. M. (1994) *J. Biol. Chem. 269,* 8255−8259.

Lin, J., & Addison, R. (1995) *J. Biol. Chem. 270,* 6942−6948.

Loo, T. W., & Clarke, D. M. (1995) *J. Biol. Chem. 270,* 843−848.

Mohraz, M., Arystarkhova, E., & Sweadner, K. J. (1994) *J. Biol. Chem. 269,* 2929−2936.

Nelson, R. M., & Long, G. L. (1989) *Anal. Biochem. 180,* 147−151.

Ohta, T., Nagano, K., & Yoshida, M. (1985) *Proc. Natl. Acad. Sci. U.S.A. 83,* 2071−2075.

Ovchinnikov, Y. A., Luneva, N. M., Arystarkhova, E. A., Gerondyan, N. M., Arzamazova, A. T., Kozhich, A. T., Nesmeyanov, V. A., & Modyanov, N. N. (1988) *FEBS Lett. 227,* 230−234.

Price, E. M., & Lingrel, J. B. (1988) *Biochemistry 27,* 8400−8408.

Shull, G. E., Schwartz, A., & Lingrel, J. B. (1985) *Nature 316,* 691−695.

Shyjan, A. W., & Levenson, R. (1989) *Biochemistry 28,* 4531−4535.

Takeyasu, K., Lemas, V., & Fambrough, D. M. (1990) *Am. J. Physiol. 259,* C619−C630.

Taylor, K. A., & Varga, S. (1994) *J. Biol. Chem. 269,* 10107−10111.

Thibault, D. (1993) *Biochemistry 32,* 2813−2821.

Towbin, H., Staehlin, T., & Gordon, J. (1979) *Proc. Natl. Acad. Sci. U.S.A. 76,* 4350−4354.

Toyoshima, C., Sasabe, H., & Stokes, D. L. (1993) *Nature 362,* 469−471.

Wilson, M. S., Niman, H., Houghton, R., Cherenson, A., Connoly, M., & Lerner, R. (1984) *Cell 37,* 767−778.

Xie, Y., & Morimoto, T. (1995) *J. Biol. Chem. 270,* 11985−11991.

Yoon, K. L., & Guidotti, G. (1994) *J. Biol. Chem. 269,* 28249−28258.

BI961851F